HONOM 2011 in Trento

DG Methods for Aerodynamic Flows: Higher Order, Error Estimation and Adaptive Mesh Refinement

Ralf Hartmann, Tobias Leicht

Institute of Aerodynamics and Flow Technology
DLR Braunschweig

11. April 2011

Research group

working on discontinuous Galerkin methods for aerodynamic flows at DLR

The current group members are:

- Dr. Ralf Hartmann
- Tobias Leicht (PhD student)
- Stefan Schoenawa (PhD student)
- Marcel Wallraff (PhD student)

former group member were:

- Dr. Joachim Held
- Florian Prill (PhD student)

Numerical results are based on:

- The DLR-PADGE code which is based on a modified version of `deal.II`.

Overview

- Higher-order discontinuous Galerkin methods
- Error estimation and adaptive mesh refinement for force coefficients
- Residual-based mesh refinement
- Numerical results for aerodynamic test cases
  - considered in the EU-project ADIGMA
    - turbulent flow around the 3-element L1T2 high-lift configuration
    - turbulent flow around the DLR-F6 wing-body configuration
  - considered in the EU-project IDIHOM
    - subsonic turbulent flow around the VFE-2 delta wing configuration
    - transonic turbulent flow around the VFE-2 delta wing configuration

DG discretization of the RANS-$k\omega$ equations

RANS and Wilcox k-ω turbulence model equations:

$$\nabla \cdot \big(F^c(\mathbf{u}) - F^v(\mathbf{u}, \nabla \mathbf{u})\big) = \mathbf{S}(\mathbf{u}, \nabla \mathbf{u})$$

Discontinuous Galerkin discretization of order $p+1$: Find $\mathbf{u}_h \in \mathbf{V}_h^p$ such that

$$\mathcal{R}(\mathbf{u}_h, \mathbf{v}_h) \equiv \int_\Omega \mathbf{R}(\mathbf{u}_h) \cdot \mathbf{v}_h \,\mathrm{d}\mathbf{x} + \sum_{\kappa \in \mathcal{T}_h} \int_{\partial\kappa \setminus \Gamma} \mathbf{r}(\mathbf{u}_h) \cdot \mathbf{v}_h^+ + \underline{\rho}(\mathbf{u}_h) : \nabla \mathbf{v}_h^+ \,\mathrm{d}s$$
$$+ \int_\Gamma \mathbf{r}_\Gamma(\mathbf{u}_h) \cdot \mathbf{v}_h^+ + \underline{\rho}_\Gamma(\mathbf{u}_h) : \nabla \mathbf{v}_h^+ \,\mathrm{d}s = 0 \quad \forall \mathbf{v}_h \in \mathbf{V}_h^p,$$

with the element residual,

$$\mathbf{R}(\mathbf{u}_h) = \mathbf{S}(\mathbf{u}_h, \nabla \mathbf{u}_h) - \nabla \cdot F^c(\mathbf{u}_h) + \nabla \cdot F^v(\mathbf{u}_h, \nabla \mathbf{u}_h),$$

and face and boundary residuals $\mathbf{r}(\mathbf{u}_h)$, $\underline{\rho}(\mathbf{u}_h)$ and $\mathbf{r}_\Gamma(\mathbf{u}_h)$, $\underline{\rho}_\Gamma(\mathbf{u}_h)$.

Error estimation with respect to target quantities

Target quantities $J(\mathbf{u})$ of interest are

- the drag, lift and moment coefficients
- pressure induced and viscous stress induced parts of the force coefficients

Error estimation with respect to target quantities

Target quantities $J(\mathbf{u})$ of interest are

- the drag, lift and moment coefficients
- pressure induced and viscous stress induced parts of the force coefficients

We want to quantity the error of the discrete function $\mathbf{u}_h$ in terms of a target quantity $J(\cdot)$, i.e. we want to quantity the error

$$J(\mathbf{u}) - J(\mathbf{u}_h)$$

Here,

- $J(\mathbf{u}_h)$ is the computed force coefficient, and
- $J(\mathbf{u})$ is the exact (but unknown) value of the force coefficient

Error estimation for single target quantities

Given a discretization: find $\mathbf{u}_h \in \mathbf{V}_{h,p}$ such that

$$\mathcal{N}(\mathbf{u}_h, \mathbf{v}_h) = 0 \quad \forall \mathbf{v}_h \in \mathbf{V}_{h,p}.$$

and a target quantity J.
Using a duality argument we obtain an error representation wrt. $J(\cdot)$:

$$\begin{aligned} J(\mathbf{u}) - J(\mathbf{u}_h) &= \mathcal{R}(\mathbf{u}_h, \mathbf{z}) := -\mathcal{N}(\mathbf{u}_h, \mathbf{z}) \\ &\approx \mathcal{R}(\mathbf{u}_h, \bar{\mathbf{z}}_h) = \sum_\kappa \bar{\eta}_\kappa. \end{aligned}$$

where $\bar{\mathbf{z}}_h$ is the solution to the discrete adjoint problem: find $\bar{\mathbf{z}}_h \in \bar{\mathbf{V}}_{h,p}$ such that

$$\mathcal{N}'[\mathbf{u}_h](\mathbf{w}_h, \bar{\mathbf{z}}_h) = J'[\mathbf{u}_h](\mathbf{w}_h) \quad \forall \mathbf{w}_h \in \bar{\mathbf{V}}_{h,p},$$

and $\bar{\eta}_\kappa$ are adjoint-based indicators which are particularly suited for the accurate and efficient approximation of the target quantity $J(\mathbf{u})$.

Residual-based mesh refinement

The DG discretization: Find $\mathbf{u}_h \in \mathbf{V}_h^p$ such that

$$\mathcal{R}(\mathbf{u}_h, \mathbf{v}_h) \equiv \int_\Omega \mathbf{R}(\mathbf{u}_h) \cdot \mathbf{v}_h \,\mathrm{d}\mathbf{x} + \sum_{\kappa \in \mathcal{T}_h} \int_{\partial\kappa \setminus \Gamma} \mathbf{r}(\mathbf{u}_h) \cdot \mathbf{v}_h^+ + \underline{\rho}(\mathbf{u}_h) : \nabla \mathbf{v}_h^+ \,\mathrm{d}s$$
$$+ \int_\Gamma \mathbf{r}_\Gamma(\mathbf{u}_h) \cdot \mathbf{v}_h^+ + \underline{\rho}_\Gamma(\mathbf{u}_h) : \nabla \mathbf{v}_h^+ \,\mathrm{d}s = 0 \quad \forall \mathbf{v}_h \in \mathbf{V}_h^p,$$

Error representation:

$$J(\mathbf{u}) - J(\mathbf{u}_h) = \mathcal{R}(\mathbf{u}_h, \mathbf{z})$$

Residual-based indicators:

$$|J(\mathbf{u}) - J(\mathbf{u}_h)| \leq \left(\sum_{\kappa \in \mathcal{T}_h} (\eta_\kappa^{\mathrm{res}})^2 \right)^{1/2}$$

$$\eta_\kappa^{\mathrm{res}} = h_\kappa \|\mathbf{R}(\mathbf{u}_h)\|_\kappa + h_\kappa^{1/2} \|\mathbf{r}(\mathbf{u}_h)\|_{\partial\kappa\setminus\Gamma} + h_\kappa^{-1/2} \|\underline{\rho}(\mathbf{u}_h)\|_{\partial\kappa\setminus\Gamma}$$
$$+ h_\kappa^{1/2} \|\mathbf{r}_\Gamma(\mathbf{u}_h)\|_{\partial\kappa\cap\Gamma} + h_\kappa^{-1/2} \|\underline{\rho}_\Gamma(\mathbf{u}_h)\|_{\partial\kappa\cap\Gamma}$$

hp-refinement with anisotropic element subdivision

hp-refinement: After having selected an element for refinement, e.g. by residual-based or adjoint-based refinement indicators, decide whether to

- split the element in subelements, i.e. use **h-refinement**, when the solution (or the adjoint solution) is smooth/regular
- increase the polynomial degree, i.e. use **p-refinement**, when the solution is non-smooth (shocks, sharp trailing edges, ...)

The decision is based on the decay of the Legendre series coefficients.

hp-refinement with anisotropic element subdivision

hp-refinement: After having selected an element for refinement, e.g. by residual-based or adjoint-based refinement indicators, decide whether to

- split the element in subelements, i.e. use **h-refinement**, when the solution (or the adjoint solution) is smooth/regular
- increase the polynomial degree, i.e. use **p-refinement**, when the solution is non-smooth (shocks, sharp trailing edges, ...)

The decision is based on the decay of the Legendre series coefficients.

Anisotropic element subdivision: After having selected an element for *h*-refinement decide upon the specific refinement case based on

- **anisotropic error estimation** or on
- an **anisotropic jump indicator**:
    - the jump of the discrete solution over element faces is associated with the approximation quality orthogonal to the face

The L1T2 high lift configuration

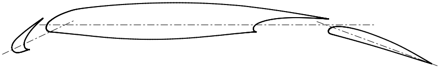

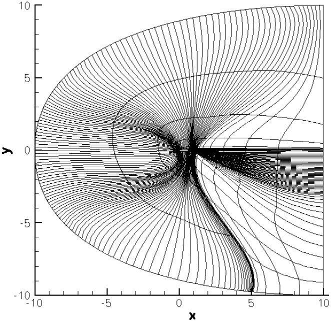

full mesh

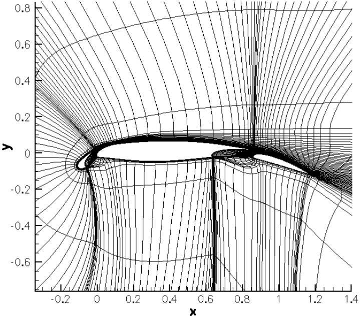

zoom of mesh

Coarse mesh of 4740 elements. Grid lines are given by polynomials of degree 4.

Turbulent flow around the L1T2 high lift configuration

Freestream conditions: $M = 0.197$, $\alpha = 20.18^\circ$ and $Re = 3.52 \times 10^6$

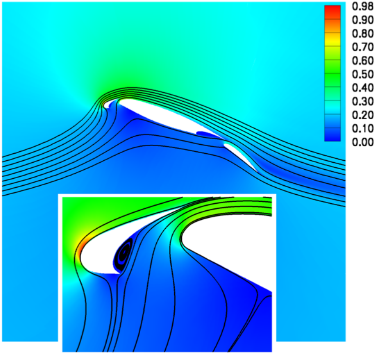

Mach number and streamlines

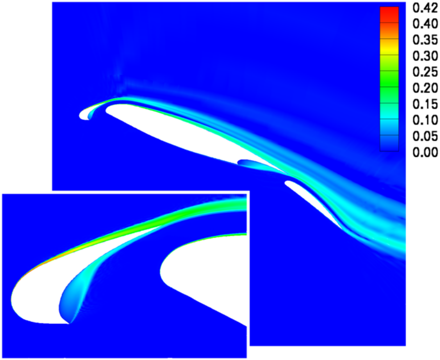

turbulent intensity

Turbulent flow around the L1T2 high lift configuration

Freestream conditions: $M = 0.197$, $\alpha = 20.18^\circ$ and $Re = 3.52 \times 10^6$

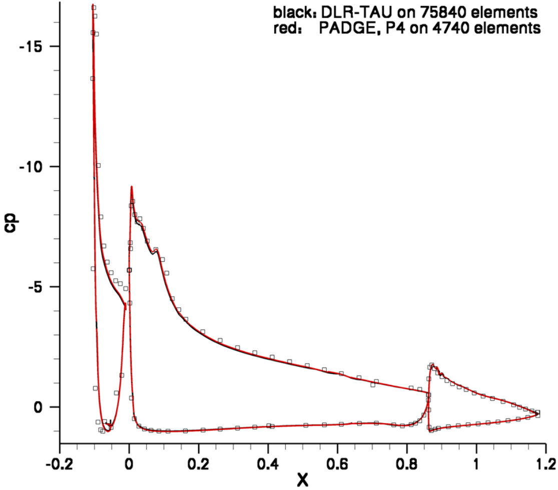

Turbulent flow around the L1T2 high lift configuration

Freestream conditions: $M = 0.197$, $\alpha = 20.18^\circ$ and $Re = 3.52 \times 10^6$

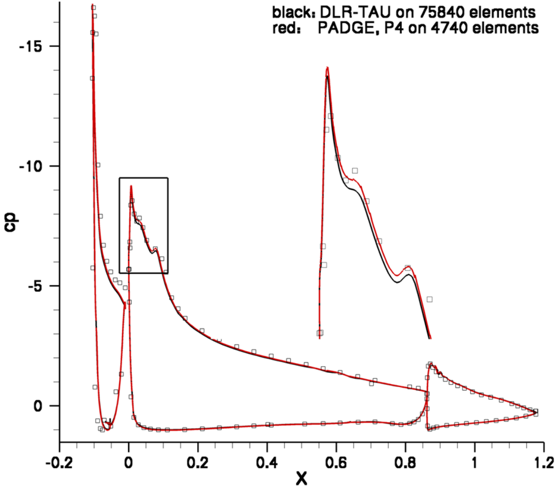

Turbulent flow around the L1T2 high lift configuration

Freestream conditions: $M = 0.197$, $\alpha = 20.18^\circ$ and $Re = 3.52 \times 10^6$

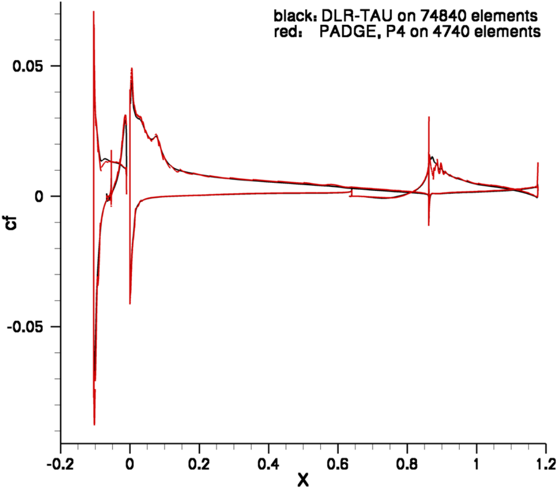

Turbulent flow around the L1T2 high lift configuration

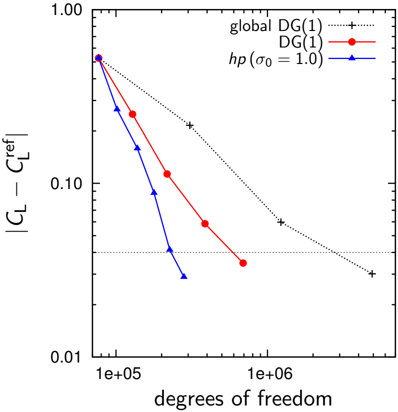

lift convergence

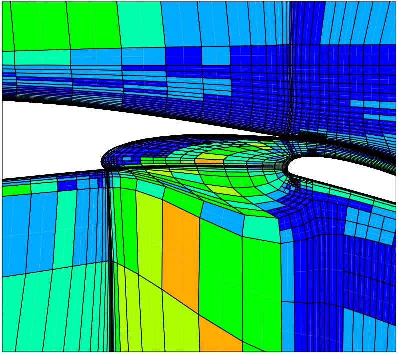

hp-adaptive mesh

Tobias Leicht

Turbulent flow around the L1T2 high lift configuration

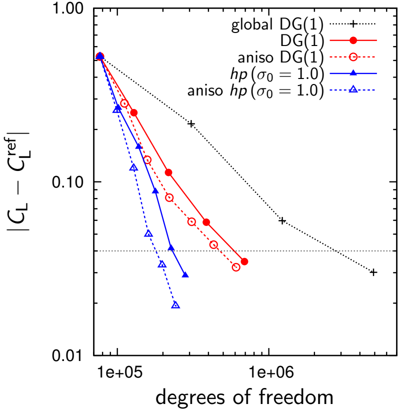

lift convergence

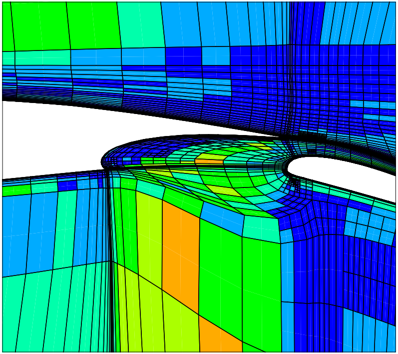

hp-adaptive mesh

Tobias Leicht

Turbulent flow around the L1T2 high lift configuration

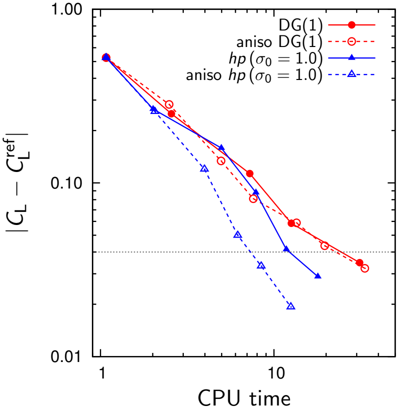

lift convergence

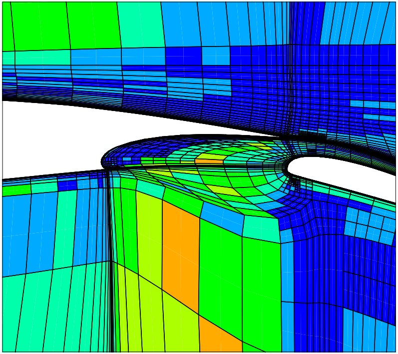

hp-adaptive mesh

Tobias Leicht

Turbulent flow around the L1T2 high lift configuration

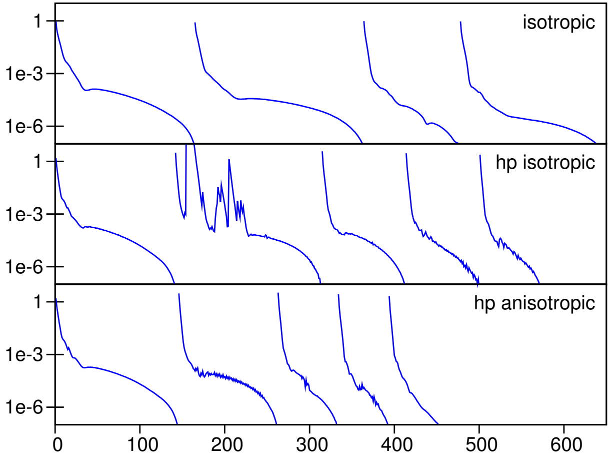

convergence: residual vs. nonlinear iterations

A suitable solution-adaptive mesh can improve the solver behavior.

Tobias Leicht

The DLR-F6 wing-body configuration without fairing

- The original mesh of 3.24×10^6 elements has been agglomerated twice.
- The elements of the coarse mesh of 50618 elements are curved based on additional points taken from the original mesh

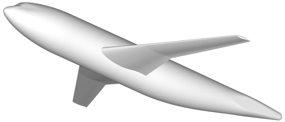

geometry

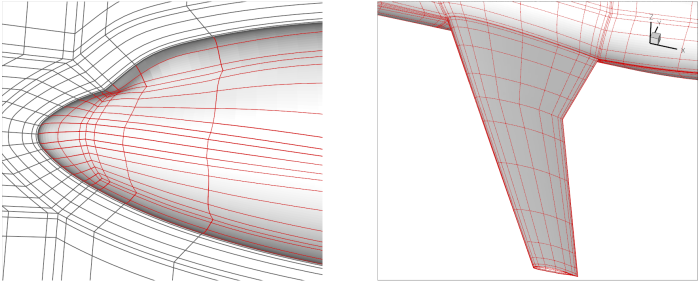

curved mesh with lines given by polynomials of degree 4

Subsonic turbulent flow around the DLR-F6 wing-body

Modification of the DPW III test case:

- $M = 0.5$ (instead of $M = 0.75$)
- $\alpha = -0.141$ (instead of target lift $C_l = 0.5$)
- $Re = 5 \times 10^6$

DG solutions on coarse mesh of 50618 curved elements.

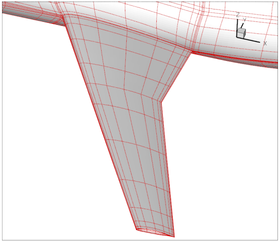

coarse mesh

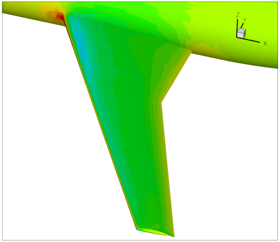

2nd order solution

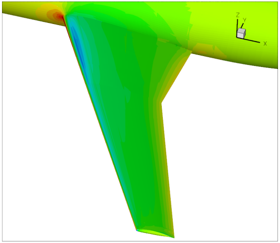

3rd order solution

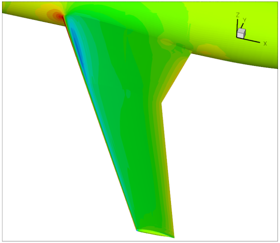

4th order solution

Subsonic turbulent flow around the DLR-F6 wing-body

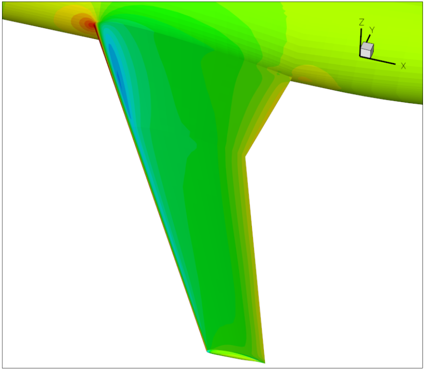

TAU on original grid

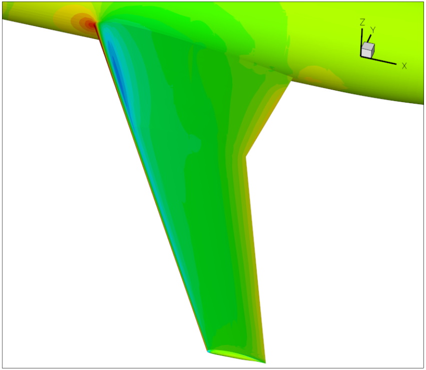

3rd order solution

after one refinement of coarse mesh

Subsonic turbulent flow around the DLR-F6 wing-body

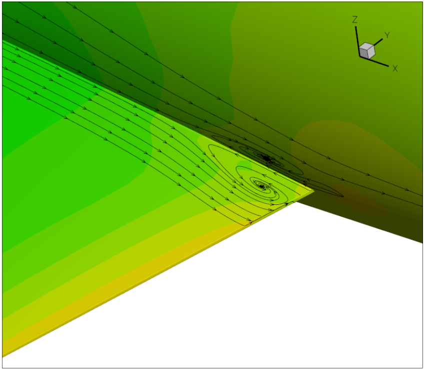

TAU on original grid

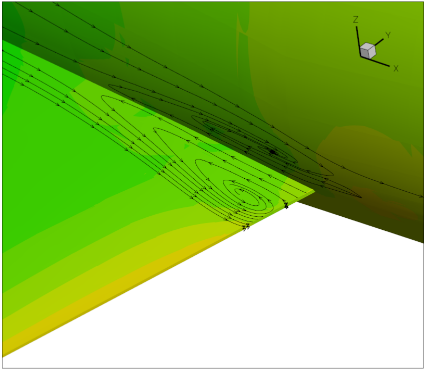

3^{rd} order solution

after one refinement of coarse mesh

Subsonic turbulent flow around the DLR-F6 wing-body

Adjoint-based refinement for C_{d}:

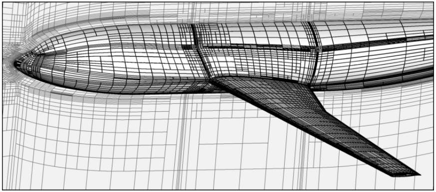

Mesh after 2 adjoint-based refinement steps

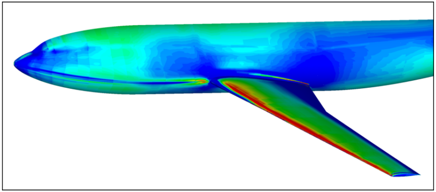

Density adjoint

Subsonic turbulent flow around the DLR-F6 wing-body

Adjoint-based refinement for C_d:

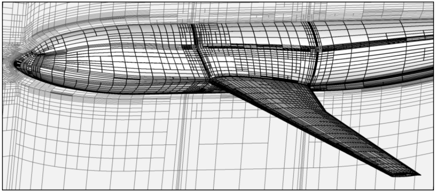

Mesh after 2 adjoint-based refinement steps

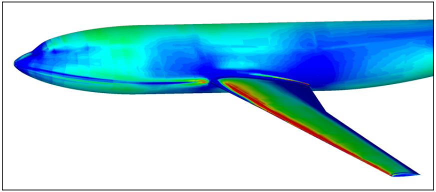

Density adjoint

Convergence of C_d
(global mesh refinement):

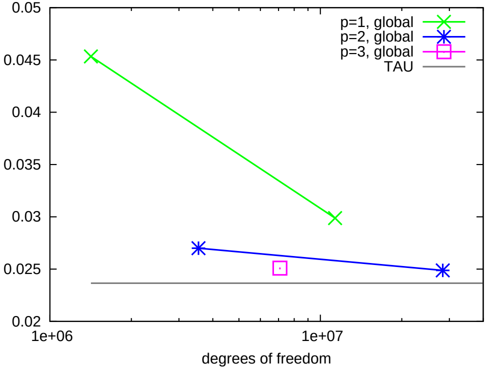

Subsonic turbulent flow around the DLR-F6 wing-body

Adjoint-based refinement for C_{d}:

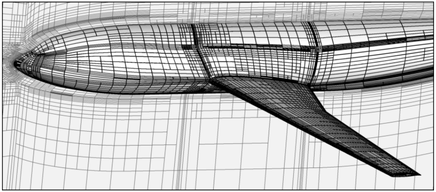

Mesh after 2 adjoint-based refinement steps

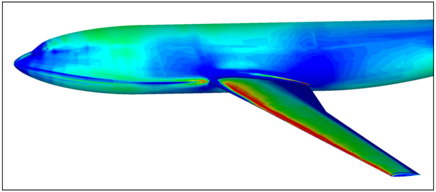

Density adjoint

Convergence of C_{d}
(global & anisotropic h-refinement):

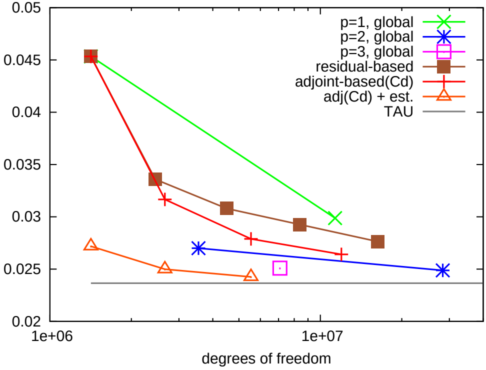

Subsonic turbulent flow around the DLR-F6 wing-body

Adjoint-based refinement for C_{d}:

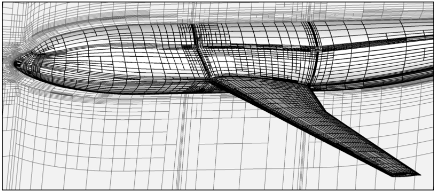

Mesh after 2 adjoint-based refinement steps

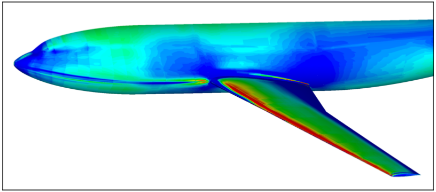

Density adjoint

Convergence of C_{d}
(global, anisotropic *h*- & *hp*-refinement):

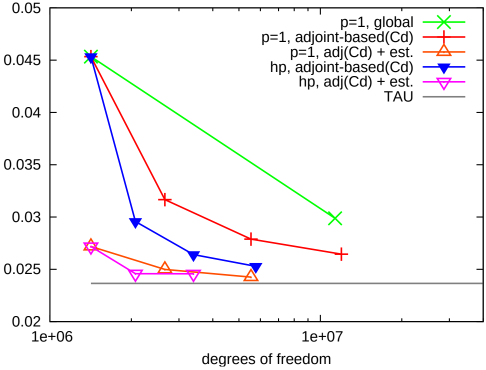

The VFE-2 delta wing with medium rounded leading edge

- The original mesh of 884 224 elements has been agglomerated twice.
- The elements of the coarse mesh of 13 816 elements are curved based on additional points taken from the original mesh

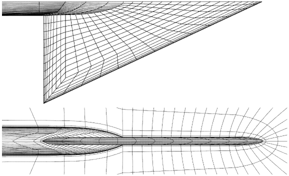

geometry

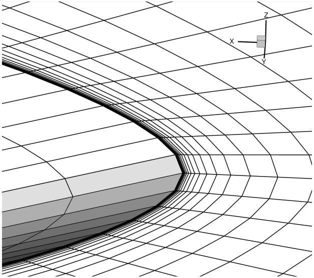

original mesh
with straight lines

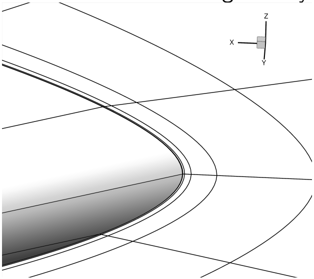

curved coarse mesh with lines
given by polynomials of degree 4

Fully turbulent flow around the VFE-2 delta wing configuration

Underlying flow case **U.1** in the EU-project **IDIHOM**

The VFE-2 delta wing with medium rounded leading edge
at two different flow conditions:

- **U.1b**: RANS-$k\omega$, **subsonic** flow at $M = 0.4$, $\alpha = 13.3^\circ$ and $Re = 3 \times 10^6$
- **U.1c**: RANS-$k\omega$, **transonic** flow at $M = 0.8$, $\alpha = 20.5^\circ$ and $Re = 2 \times 10^6$

Subsonic flow around the VFE-2 delta wing

U.1b: Fully turbulent flow at $M = 0.4$, $\alpha = 13.3^\circ$ and $Re = 3 \times 10^6$

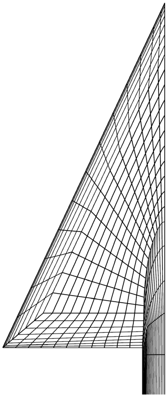

coarse mesh with

13 816 curved elements

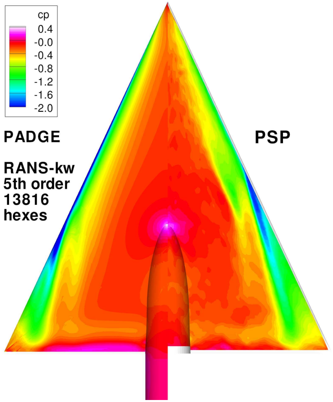

c_p distribution

5^{th} order solution vs. experiment (PSP)

Subsonic flow around the VFE-2 delta wing

U.1b: Fully turbulent flow at $M = 0.4$, $\alpha = 13.3^\circ$ and $Re = 3 \times 10^6$

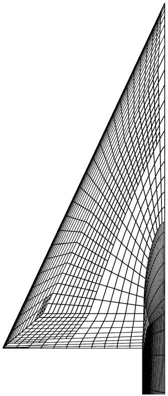

residual-based refined mesh with

84 348 curved elements

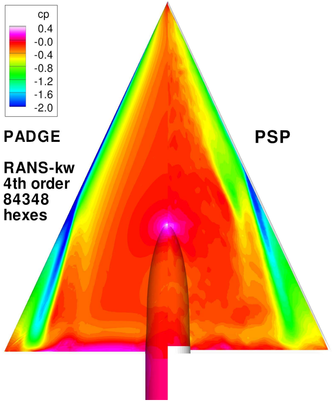

c_p distribution

4^{th} order solution vs. experiment (PSP)

Subsonic flow around the VFE-2 delta wing

U.1b: Fully turbulent flow at $M = 0.4$, $\alpha = 13.3^\circ$ and $Re = 3 \times 10^6$

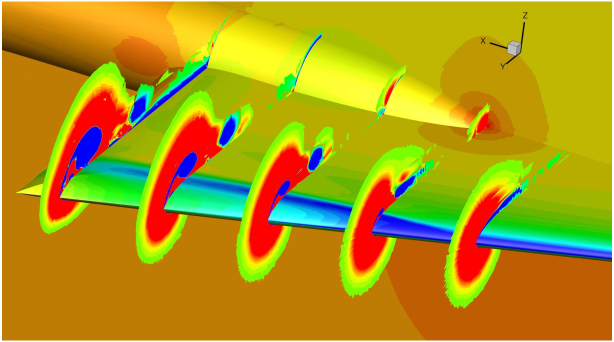

4^{th}-order solution on residual-based refined mesh with 84 348 curved elements

Subsonic flow around the VFE-2 delta wing

U.1b: Fully turbulent flow at $M = 0.4$, $\alpha = 13.3^\circ$ and $Re = 3 \times 10^6$

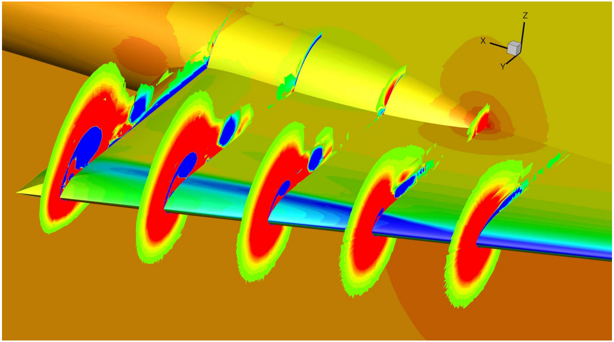

4^{th}-order solution on residual-based refined mesh with 84 348 curved elements

2^{nd}-order solution on residual-based refined mesh with 562 892 curved elements

Fully turbulent flow around the VFE-2 delta wing configuration

Underlying flow case **U.1** in the EU-project **IDIHOM**

The VFE-2 delta wing with medium rounded leading edge
at two different flow conditions:

- **U.1b**: RANS-$k\omega$, **subsonic** flow at $M = 0.4$, $\alpha = 13.3^\circ$ and $Re = 3 \times 10^6$
- **U.1c**: RANS-$k\omega$, **transonic** flow at $M = 0.8$, $\alpha = 20.5^\circ$ and $Re = 2 \times 10^6$
  requires shock capturing

Shock-capturing based on artificial viscosity (1)

$$\mathcal{N}_{sc}(\mathbf{u}_h, \mathbf{v}) \equiv \sum_\kappa \int_\kappa \varepsilon(\mathbf{u}_h) \nabla \mathbf{u}_h : \nabla \mathbf{v} d\mathbf{x} \equiv \sum_\kappa \int_\kappa \varepsilon_{klm}(\mathbf{u}_h) \partial_{x_l} u_h^m \, \partial_{x_k} v^m \, d\mathbf{x},$$

- For the compressible Navier-Stokes equations (2nd order DG discretization), [1]

$$\varepsilon_{klm}(\mathbf{u}_h) = C_\varepsilon \, \delta_{kl} h_k^{2-\beta} \, \mathcal{R}_m(\mathbf{u}_h), \quad k, l = 1, \dots, d \, , m = 1, \dots, n,$$

$$\mathcal{R}_m(\mathbf{u}_h) = \sum_{q=1}^n |R_q(\mathbf{u}_h)|, \quad m = 1, \dots, n,$$

where $\mathbf{R}(\mathbf{u}_h) = (R_q(\mathbf{u}_h), q = 1, \dots, n)$ is the residual of the PDE given by

$$\mathbf{R}(\mathbf{u}_h) = -\nabla \cdot (\mathcal{F}^c(\mathbf{u}_h) - \mathcal{F}^v(\mathbf{u}_h, \nabla \mathbf{u}_h)) \, .$$

[1] R. Hartmann. Adaptive discontinuous Galerkin methods with shock-capturing for the compressible Navier-Stokes equations. *Int. J. Numer. Meth. Fluids*, 51(9–10):1131–1156, 2006.

Shock-capturing based on artificial viscosity (2)

$$\mathcal{N}_{sc}(\mathbf{u}_h, \mathbf{v}) \equiv \sum_\kappa \int_\kappa \varepsilon(\mathbf{u}_h) \nabla \mathbf{u}_h : \nabla \mathbf{v} dx \equiv \sum_\kappa \int_\kappa \varepsilon_{klm}(\mathbf{u}_h) \partial_{x_l} u_h^m \, \partial_{x_k} v^m \, d\mathbf{x},$$

- For the RANS-$k\omega$ equations (2nd and higher order discretization),[2]

$$\varepsilon_{klm}(\mathbf{u}_h) = C_\varepsilon \, b_k b_l h_\kappa^2 \, f_p(\mathbf{u}_h) \, \frac{|R_p(\mathbf{u}_h)| + |s_p(\mathbf{u}_h^+, \mathbf{u}_h^-)|}{p}, \qquad \mathbf{b} = \frac{\nabla p}{|\nabla p| + \varepsilon'}$$

$$R_p(\mathbf{u}_h) = \sum_{m=1}^{d+2} \frac{\partial p}{\partial u_m} R_m(\mathbf{u}_h), \qquad s_p(\mathbf{u}_h^+, \mathbf{u}_h^-) = \sum_{m=1}^{d+2} \frac{\partial p}{\partial u_m} s_m(\mathbf{u}_h^+, \mathbf{u}_h^-),$$

with

$$\mathbf{R}(\mathbf{u}_h) = -\nabla \cdot \mathcal{F}^c(\mathbf{u}_h),$$

$$\int_\kappa s_m(\mathbf{u}_h^+, \mathbf{u}_h^-) \, \mathbf{v}_h \, d\mathbf{x} = \int_{\partial\kappa} \left(\mathcal{H}(\mathbf{u}_h^+, \mathbf{u}_h^-, \mathbf{n}^-) - \mathcal{F}^c(\mathbf{u}_h^+) \cdot \mathbf{n}^+ \right)_m \mathbf{v}_h \, ds$$

---

[2] F. Bassi et. al. Very high-order accurate Discontinuous Galerkin Computation of transonic turbulent flows on Aeronautical configurations, *ADIGMA*, NNFMMD 113, 2010.

Shock-capturing based on artificial viscosity (combines 1 and 2)

$$\mathcal{N}_{sc}(\mathbf{u}_h, \mathbf{v}) \equiv \sum_{\kappa} \int_{\kappa} \varepsilon(\mathbf{u}_h) \nabla \mathbf{u}_h : \nabla \mathbf{v} d\mathbf{x} \equiv \sum_{\kappa} \int_{\kappa} \varepsilon_{klm}(\mathbf{u}_h) \partial_{x_l} u_h^m \, \partial_{x_k} v^m \, d\mathbf{x},$$

- For the RANS-$k\omega$ equations (2nd and higher order discretization)

$$\varepsilon_{klm}(\mathbf{u}_h) = C_\varepsilon \, \delta_{kl} \tilde{h}_k^2 \, f_p(\mathbf{u}_h) \, \frac{|R_p(\mathbf{u}_h)|}{p}, \quad k, l = 1, \dots, d \, , m = 1, \dots, d + 2,$$

$$R_p(\mathbf{u}_h) = \sum_{m=1}^{d+2} \frac{\partial p}{\partial u_m} \, R_m(\mathbf{u}_h),$$

$$\mathbf{R}(\mathbf{u}_h) = \mathbf{S}(\mathbf{u}_h, \nabla \mathbf{u}_h) - \nabla \cdot F^c(\mathbf{u}_h) + \nabla \cdot F^v(\mathbf{u}_h, \nabla \mathbf{u}_h),$$

$$\tilde{h}_i = h_i / (\mathrm{degree} + 1),$$

where h_i is the dimension of the element κ in the x_i-coordinate direction

Transonic flow around the VFE-2 delta wing

U.1c: Fully turbulent flow at $M = 0.8$, $\alpha = 20.5^\circ$ and $Re = 2 \times 10^6$

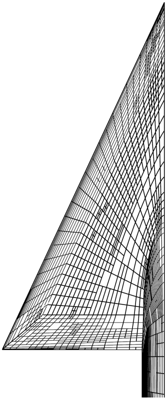

refined mesh with

201 259 curved elements

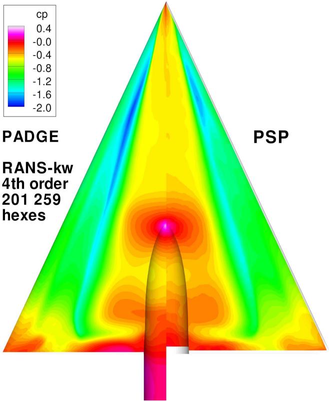

c_p distribution

4[th] order solution vs. experiment (PSP)

Transonic flow around the VFE-2 delta wing

U.1c: Fully turbulent flow at $M = 0.8$, $\alpha = 20.5^\circ$ and $Re = 2 \times 10^6$

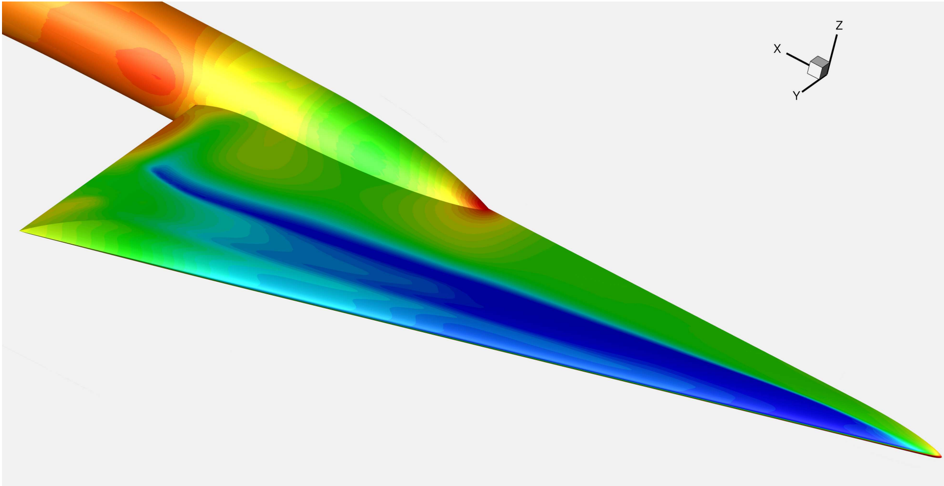

4^{th}-order solution on residual-based refined mesh with 201 259 curved elements

Transonic flow around the VFE-2 delta wing

U.1c: Fully turbulent flow at $M = 0.8$, $\alpha = 20.5^\circ$ and $Re = 2 \times 10^6$

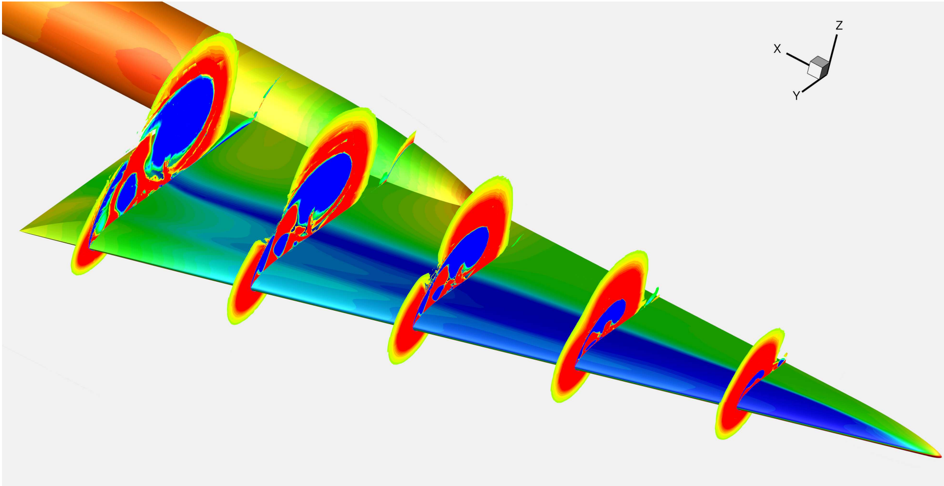

4^{th}-order solution on residual-based refined mesh with 201 259 curved elements

Transonic flow around the VFE-2 delta wing

U.1c: Fully turbulent flow at $M = 0.8$, $\alpha = 20.5^\circ$ and $Re = 2 \times 10^6$

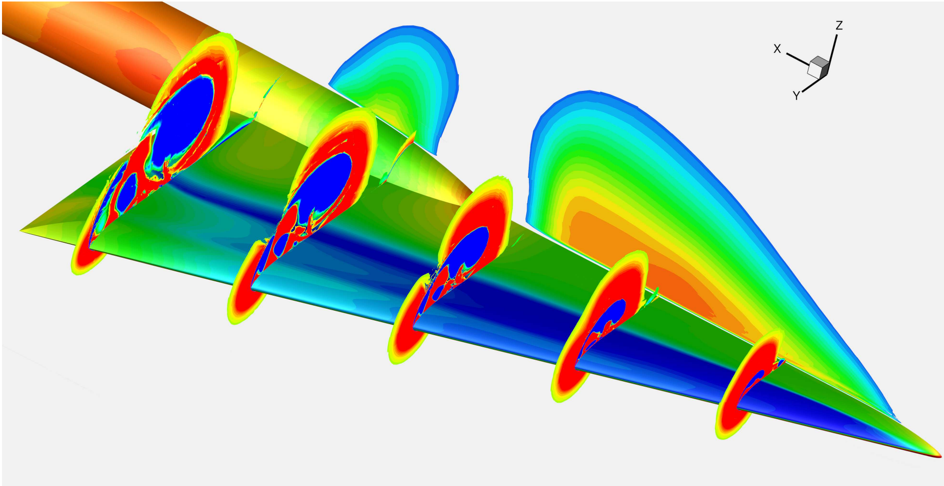

4^{th}-order solution on residual-based refined mesh with 201 259 curved elements

Transonic flow around the VFE-2 delta wing

U.1c: Fully turbulent flow at $M = 0.8$, $\alpha = 20.5^\circ$ and $Re = 2 \times 10^6$

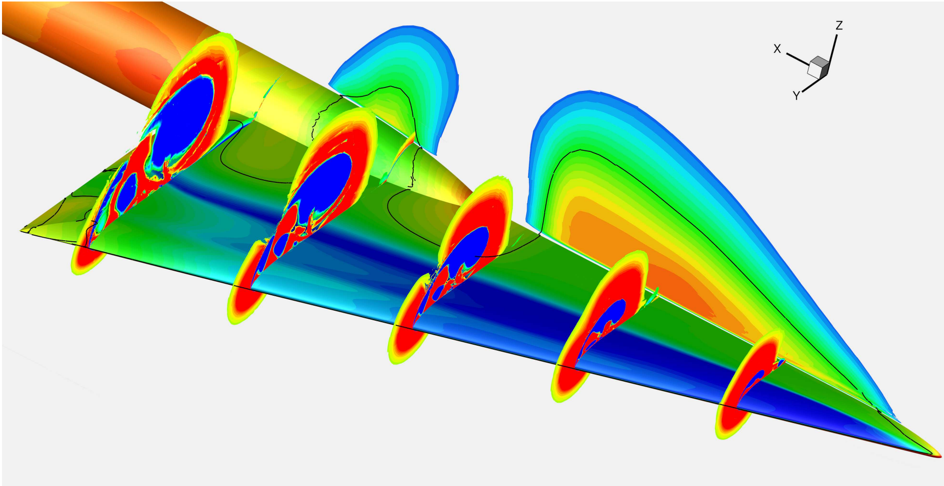

4^{th}-order solution on residual-based refined mesh with 201 259 curved elements

Transonic flow around the VFE-2 delta wing

U.1c: Fully turbulent flow at $M = 0.8$, $\alpha = 20.5^\circ$ and $Re = 2 \times 10^6$

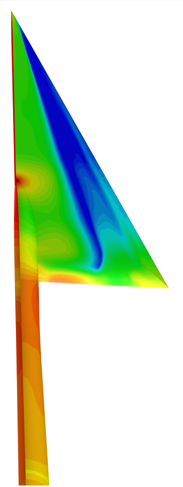

c_p

Transonic flow around the VFE-2 delta wing

U.1c: Fully turbulent flow at $M = 0.8$, $\alpha = 20.5^\circ$ and $Re = 2 \times 10^6$

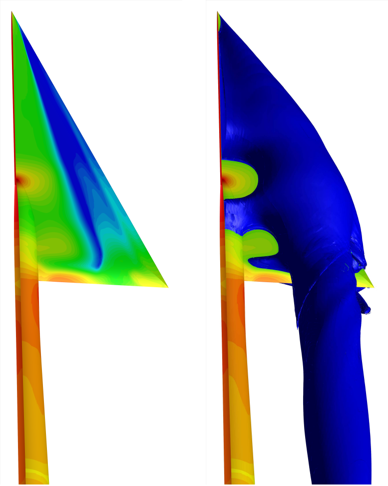

c_p and $M = 1$ isosurface

Transonic flow around the VFE-2 delta wing

U.1c: Fully turbulent flow at $M = 0.8$, $\alpha = 20.5^\circ$ and $Re = 2 \times 10^6$

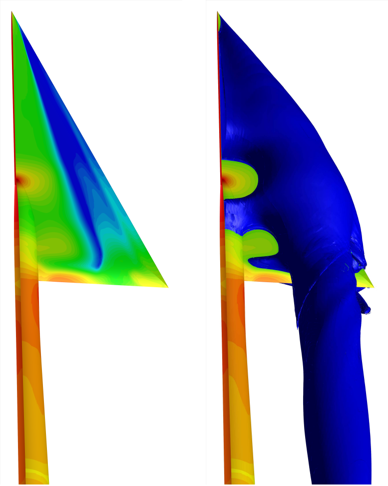

c_p and $M = 1$ isosurface

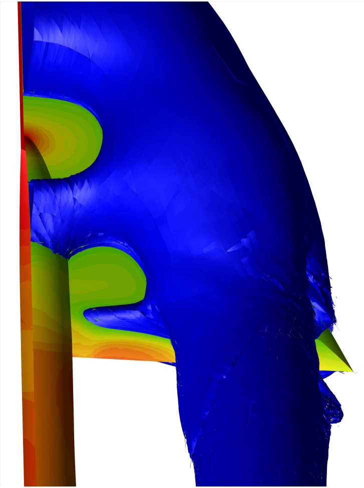

zoom of $M = 1$ isosurface

Summary

- Higher-order discontinuous Galerkin methods
- Error estimation and adaptive mesh refinement for force coefficients
- Residual-based mesh refinement
- Numerical results for aerodynamic flows around
  - the 3-element L1T2 high-lift configuration
  - the DLR-F6 wing-body configuration
  - the VFE-2 delta wing configuration (subsonic and transonic)

Computations have been performed with the DLR-PADGE code

Thank you